

Polarization-dependent $C(K)$ near-edge x-ray-absorption fine structure of graphite

R. A. Rosenberg,* P. J. Love, and Victor Rehn

Michelson Laboratory, Naval Weapons Center, China Lake, California 93555

(Received 1 October 1985)

Photoabsorption spectra of graphite at photon energies between 275 and 345 eV are presented. The spectra show dramatic changes as the angle, α , between the Poynting vector and the surface normal is varied. By varying α , one is able to select the symmetry of the final state (σ or π). Using this information, we are able to assign the spectral features to states predicted by published band-structure calculations.

I. INTRODUCTION AND SUMMARY

Near-edge x-ray-absorption fine structure (NEXAFS) measurements show great promise as a site-specific probe of electronic and geometric structure. Recently, the angular dependence of these spectra has been used to determine the orientation of chemisorbed molecules on surfaces, while the peak positions have been used to determine bond distances.^{1,2} The angular variations are a consequence of the fixed orientation of the adsorbed molecules, which results in final states of σ symmetry being selected when the polarization vector \mathbf{E} is aligned with the bond axis, while states of π symmetry are probed when the \mathbf{E} is perpendicular to the intermolecular axis. Polarization-dependent x-ray absorption has also been used to probe the structure of the layered compounds $2H\text{-WSe}_2$ and $1T\text{-TaS}_2$.³

Graphite, with its layered structure and large interlayer separation, is often modeled as a two-dimensional solid. As a consequence, it has been the subject of a great deal of experimental and theoretical effort. In addition, a knowledge of the properties of graphite is a starting point for understanding intercalated graphite, which is a field of very active research.⁴ The two-dimensional nature of graphite results in a strong directionality of the orbitals: σ orbitals lie within the basal plane, while π orbitals are directed perpendicular to the basal plane. By using tunable, polarized synchrotron light, it is possible to excite final states of a specific symmetry from K -shell initial states. When the \mathbf{E} vector lies within the basal plane, σ final states are selected, while when the \mathbf{E} vector is perpendicular to the plane, states of π symmetry are excited. By monitoring the angular variations of the spectral features of the $C(K)$ NEXAFS spectrum, we have determined the symmetry of the final states. This has made it possible to assign these spectral features to particular Brillouin-zone regions in the theoretical band structure of graphite.

Previous studies of the graphite $C(K)$ -edge NEXAFS spectrum have been performed on non-single-crystal samples⁵ or have utilized electrons as an excitation source.^{6,7} There have been several calculations of the band structure of graphite.⁸⁻¹⁰ For the purposes of this work, we found the calculation of Willis, Fitton, and Painter⁹ to be the most useful.

We present the first polarization-dependent photoabsorption study of $C(K)$ excitation in graphite.¹¹ The spectra show dramatic variations in peak intensities and positions as the angle α between the Poynting vector of the light and the surface normal is varied. These differences result from excitation to final states of σ or π symmetry, each of which has different angular properties. The initial peak has been shown to be a $C(1s)$ to π excitation by the linear dependence of the peak intensity versus $\sin^2\alpha$. Higher-lying peaks have been identified with specific-symmetry bands in a theoretical band-structure calculation and the theoretical density of states (DOS) has been used to reproduce many of the spectral features.

II. EXPERIMENTAL

The experiments were performed on beam line I-1 at the Stanford Synchrotron Radiation Laboratory. This beam line utilizes a "grasshopper" monochromator with fixed (20- μm) entrance and exit slits and a 1200 mm^{-1} grating. The theoretical photon-energy resolution is roughly 1 eV at 300 eV.

The highly oriented pyrolytic graphite (HOPG) sample was obtained from Union Carbide. The sample was mounted on a precision XYZ Θ manipulator with the c axis normal to the surface and introduced into an ultrahigh-vacuum chamber without further cleaning. After evacuating the chamber, the sample was heated to approximately 200°C to remove any weakly bound adsorbates (e.g., H_2O). Cleanliness of the sample was determined by noting the lack of any perceptible photoabsorption edge jump at the $O(K)$ edge. The base pressure of the chamber was 2×10^{-10} torr.

The photoabsorption spectra were taken by recording the total electron yield (TEY) from the sample as a function of photon energy and angle α . At these photon energies, the TEY signal is proportional to the photoabsorption coefficient.¹² The electrons were detected by a tandem array of microchannel plates (MCP) located behind a series of high-transmission grids. For these measurements, all of the grids and the front of the MCP's were operated at a potential of 140 V, while the back of the MCP was at 1400 V. The resulting analog current was converted to a digital signal and stored in a computer. All spectra were normalized to the photon flux by simul-

taneously recording the TEY signal from an *in situ* copper-coated mesh placed in the incident photon beam.

The photon energy was calibrated using the positions of two minima (284.7 and 291.0 eV) (Ref. 1) in the monochromator transmission function. We estimate the error in the energy calibration to be ± 0.5 eV. The angle of the light with respect to the sample was calibrated by noting the manipulator setting at which zero-order light was reflected through a known angle. The uncertainty in incident angle is $\pm 2^\circ$. The polarization of the light has been estimated to be 86% in the horizontal plane.¹

III. RESULTS AND DISCUSSION

TEY spectra between 275 and 345 eV are shown in Fig. 1, as a function of the angle α between the Poynting vector and the surface normal (c axis). The spectral features arise from transitions of a C($1s$) electron to states of σ or π symmetry. Dipole selection rules may be used to understand the angular dispersion of the peak intensities:

$$1s \rightarrow \sigma \text{ for } \mathbf{E} \perp \mathbf{c}, \quad (1)$$

$$1s \rightarrow \pi \text{ for } \mathbf{E} \parallel \mathbf{c}. \quad (2)$$

The most dramatic result of Fig. 1 is the decrease in in-

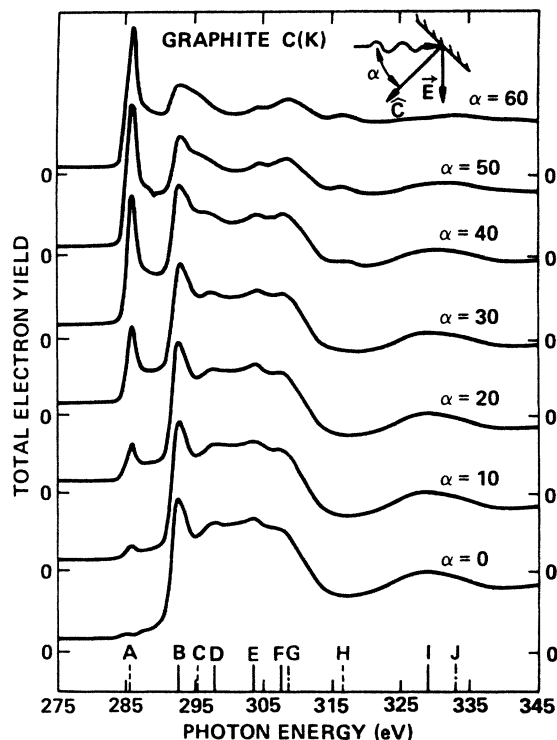


FIG. 1. C(K)-edge photoabsorption spectra of single-crystal graphite at various angles of incidence α , between the surface normal and the Poynting vector of the light. At the bottom of the figure are lines showing the peak energies: dashed lines represent states of π symmetry, while solid lines represent states of σ symmetry. States whose symmetry could not be determined are represented by dashed-dotted lines. The monochromator photon-energy calibration is estimated to be accurate to ± 0.5 eV.

tensity of peak *A* at 285.5 eV as α is decreased. For $\alpha=0^\circ$, this peak has virtually disappeared. This angular dependence allows us to unequivocally assign this peak to a $1s$ to π transition. This transition is analogous to the $1s$ to π^* transition observed in many molecular systems.^{1,13} The residual intensity of the peak at $\alpha=0^\circ$ is probably due to a combination of sample misalignment and incomplete polarization of the light.

Previous electron-energy-loss spectra (EELS) of crystalline graphite^{6,7} and photoabsorption studies of polycrystalline graphite⁵ have also recorded the peak at 285.5 eV and assigned it to a $1s \rightarrow \pi$ excitation. The EELS study of Mele and Ritsko⁷ was complemented by a scattering-theory calculation of the line shape of this peak, which predicted a logarithmic singularity in the density of states, appearing as a kink on the high-energy side (286.6 eV) of the peak in their spectrum. This feature is also evident as a shoulder near 287 eV in the data of Fig. 1.

For electric dipole transitions excited by polarized light, the intensity varies as $\sin^2\alpha$. Therefore, in single-crystal graphite, the intensity of a pure $1s \rightarrow \pi$ transition should be proportional to $\sin^2\alpha$, while the intensity of a pure $1s \rightarrow \sigma$ transition should be proportional to $\cos^2\alpha$. The HOPG sample used in this work differs from a perfect single crystal only in the rotation of the basal planes with respect to one another. This property should have no effect on the polarization dependence of the photoabsorption with respect to the angle α , but would be important if angular distributions were being determined in the basal plane. In Fig. 2 we have plotted the intensity of the peak *A* as a function of $\sin^2\alpha$. The peak intensities were calculated by normalizing to the pre-edge intensity by

$$I = (\mu - \mu_0) / \mu_0, \quad (3)$$

where I is the relative intensity, μ is the peak height, and μ_0 is the pre-edge intensity. The linearity of the data shown in Fig. 2 confirms the assignment of the first peak to a $1s \rightarrow \pi$ transition.

By monitoring the angular variations of the other spectral features in Fig. 1, we may gain insight into the symmetries of the final states. In the $\alpha=0^\circ$ spectrum, only final states of σ symmetry are excited, while states of π symmetry may be excited as α is increased. At the bottom of Fig. 1 is a representation of the final-state symmetries deduced from the angular variation of the peaks. The dashed lines represent states of π symmetry, while the

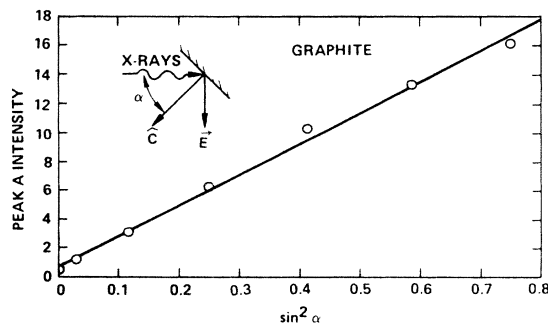


FIG. 2. Relative intensity of peak *A* (Fig. 1) as a function of $\sin^2\alpha$.

solid lines indicate states of σ symmetry. For peaks *G* and *J*, an unambiguous determination of the symmetry was not possible, so they are represented by a dashed-dotted line. Inadequate energy resolution and uncertain normalization result in uncertainties in the peak intensities. These uncertainties limit the accuracy and utility of plots of intensity versus $\sin^2\alpha$ for the other spectral features in Fig. 1. Thus, assignments *B* thru *J* at the bottom of Fig. 1 are based solely on the qualitative angular dependence of the corresponding spectral features.

On the left side of Fig. 3, we have reproduced the graphite band-structure calculation of Willis, Fitton, and Painter.⁹ On the right side of Fig. 3 we have transposed the graphical representation of the final-state symmetries deduced from Fig. 1. The lowest-energy state (peak *A*, 285.5 eV) is aligned with the lowest-lying state of symmetry π_0 , which crosses *Q* at 2 eV above the Fermi level E_F in agreement with the assignment from previous photoabsorption work on graphite.⁵ Since the initial state, the $C(1s)$ level is essentially flat (the band has very little dispersion); the only transitions allowed by dipole selection rules are to maxima or minima in the band structure (M_0 or M_3 transitions). By comparing the peak positions and symmetries deduced from Fig. 1 to the band structure of Fig. 3, we are able to assign many of the peaks to excitations to particular states in specific Brillouin-zone regions. These assignments are summarized in Table I. For comparison, we have also listed peak positions from other studies of graphite.

The large number of bands makes precise assignment difficult; however, by monitoring the angular dispersion of the peaks, we are able to resolve many features that

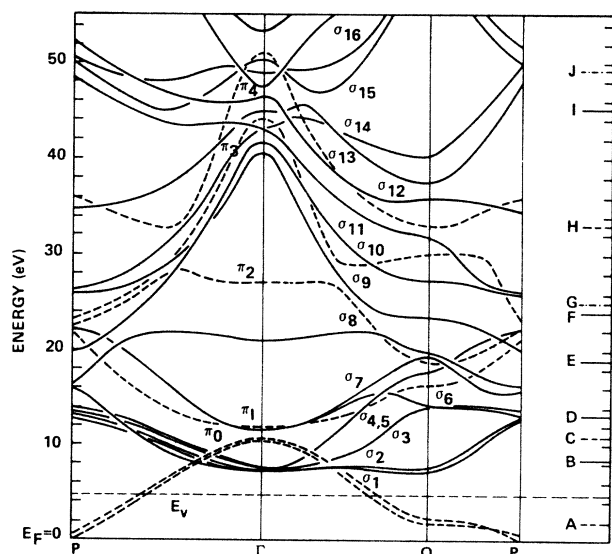


FIG. 3. Band structure of graphite reproduced from a calculation by Willis, Fitton, and Painter (Ref. 9) (left). The graphical representation of the peak positions and symmetries from the bottom of Fig. 1 have been transposed to the right of the band diagram. The energy scale was aligned so that peak *A* corresponds to the lowest-lying state of π symmetry π_0 , near *Q* in the Brillouin zone, at 2 eV above the Fermi energy E_F . The vacuum level is indicated by a dashed line.

TABLE I. Energies and assignments of peaks in the $C(K)$ -edge excitation spectrum of single-crystal graphite.

Peak	Energy (eV)			Final-state band and Brillouin-zone region
	This work ^a	Ref. 5	Ref. 9 ^b	
<i>A</i>	285.5	285		π_0 near <i>Q</i>
<i>B</i>	292.5	293	292.4	σ_1, σ_2 : $\Gamma \rightarrow Q$
<i>C</i>	295.5			π_0 or π_1 near Γ
<i>D</i>	297.8		296.9	σ_3 - σ_6 : $Q \rightarrow P$
<i>E</i>	303.5	302	303.9	σ_7 near <i>Q</i>
<i>F</i>	307.5		306.9	σ_9 near <i>Q</i>
<i>G</i>	308.5			
<i>H</i>	316.5	316.5		π_4 near <i>Q</i>
<i>I</i>	329	325		
<i>J</i>	333			

^aEnergy uncertainty is ± 0.5 eV.

^bThese energies were obtained by adding the binding energy of the $C(1s)$ electron in graphite (284.7 eV) (Ref. 14) to the energies given in Ref. 9.

were ambiguous in previous studies. For example, we observe three features (*B, C, D*) in the 292–298-eV region, where previous workers have only reported one. Our peak positions compare reasonably well with previous photoabsorption studies of polycrystalline graphite⁵ and secondary-electron-emission (SEE) work on crystalline graphite.⁹ In order to compare the SEE data, it is necessary to add the binding energy of the $C(1s)$ electron in graphite (284.7 eV) (Ref. 14) to the SEE results to obtain the values in Table I. Because $\pi_0(Q)$ lies below the vacuum energy E_v , peak *A* was not observed in the SEE work. The major differences are in the position of peaks *E* and *I* in the polycrystalline graphite data, which may be attributed to the differences in samples. The EELS spectrum of Kincaid, Meixner, and Platzman⁶ is similar to the $\alpha=50^\circ$ spectrum (Fig. 1), but peak energies were not given. A momentum transfer (q) dependence of the peak-*A* intensity was observed in the EELS study, but no q dependence was reported for the other peaks.⁶

In assigning the peaks to features in the density of states deduced from a one-electron calculation of the band structure, we are neglecting possible contributions from extended x-ray-absorption fine structure (EXAFS) and multiple scattering of the outgoing electron. EXAFS oscillations may contribute to the higher-energy structure, peaks *I* and *J*, while multiple scattering is expected to be important at lower energies. Since multiple-scattering calculations have not been applied to the graphite system, it is not possible to determine how such effects may influence the spectra of Fig. 1.

Recent experimental work has indicated that, in certain cases, there is a linear dependence between the position of σ shape resonances observed in gas-phase NEXAFS spectra and the intermolecular bond length.² For C—C bonds, this model predicts that for a C—C bond length of 1.42 Å (the C—C bond length in graphite), a σ shape resonance should be observed at an energy 7.3 eV above the $C(1s)$ binding energy (284.7 eV),¹⁴ or at an excitation energy of 292 eV. It is interesting to note that this energy is very close to the 292.5-eV excitation energy of peak *B*

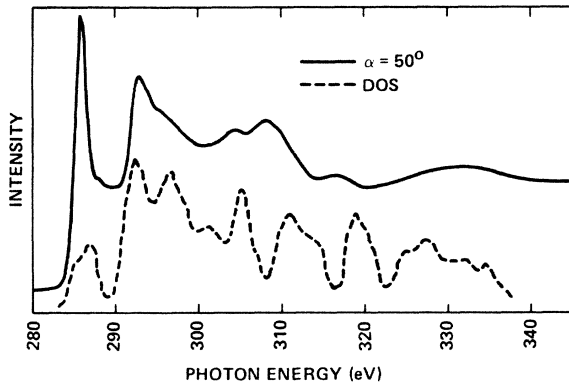


FIG. 4. Solid curve: experimental ($\alpha=50^\circ$) photoabsorption spectrum. Dashed curve: smoothed theoretical density of states (Ref. 9).

(Table I), which we determined to have σ symmetry.

In Fig. 4 the smoothed theoretical one-electron density of states of Willis, Fitton, and Painter⁹ is compared to the $\alpha=50^\circ$ spectrum, where σ and π transitions are nearly equally possible. The energy scale was set by aligning the 285.5-eV experimental peak with the DOS feature at 2 eV above E_F , corresponding to excitation to the π_0 band. The 50° spectrum was chosen because it is closest to $\alpha=54.7^\circ$, the angle at which the peak intensities should be independent of the angular asymmetry parameter β according to

$$\mu(\alpha) = (\mu_0/4\pi) [1 + \frac{1}{2}\beta(3\cos^2\alpha - 1)], \quad (4)$$

where μ_0 is the integrated photoabsorption cross section and β is an asymmetry parameter. At $\alpha=54.7^\circ$, $3\cos^2\alpha - 1 = 0$ and $\mu = \mu_0/4\pi$. The histogram DOS of Ref. 9 was smoothed to more closely simulate the experimental spectrum. The overall features of the DOS are reproduced in the experimental data, although peak energies and intensities are different. Energy differences are probably due to differences in relaxation energy for the various final states, which the one-electron DOS does not take into account. The theoretical work of Mele and

Ritsko⁷ has shown that the relaxation energy for the initial excitation, peak A, is about 2 eV; calculations were not performed for any of the higher-lying states.⁷ Since the initial excitation has been identified as a localized Frenkel-like exciton,⁷ while the higher-lying excitations are to delocalized conduction-band states, it seems likely that relaxation will not affect the higher-lying states as much as the initial excitation. Therefore, the higher-lying DOS features will appear at lower energies relative to the experimental spectrum, when the C(1s) $\rightarrow \pi_0$ (peak A) excitation energy is used as a reference point. The data of Fig. 4 indicate this type of behavior.

IV. CONCLUSIONS

The results presented here show the wealth of information available in polarization-dependent core-level photoabsorption studies on highly oriented systems such as graphite. If this information is to be fully utilized, more theoretical effort is needed in this area. As a starting point a calculation, including relaxation, of the partial density of σ and π states is needed. This would allow one to more accurately model the experimental data. In addition, multiple-scattering calculations, which have shown great promise when applied to other materials,¹⁵ could be used to understand this model system.

ACKNOWLEDGMENTS

We would like to thank Al Green for supplying the graphite sample and Carol Baker for assisting in the data acquisition. This work was supported by the National Science Foundation, by the U.S. Naval Weapons Center Independent Research Fund, and by the U.S. Office of Naval Research. Experiments were conducted at the Stanford Synchrotron Radiation Laboratory, which is supported by the U.S. Department of Energy (Office of Basic Energy Sciences), by the National Science Foundation (Division of Materials Research), and by the National Institutes of Health (Biotechnology Resource Program, Division of Research Resources).

*Present address: Synchrotron Radiation Center, University of Wisconsin-Madison, 3725 Schneider Drive, Stoughton, WI 53589.

¹J. Stöhr and R. Jaeger, Phys. Rev. B **26** 4111 (1982).

²F. Sette, J. Stöhr, and A. P. Hitchcock, Chem. Phys. Lett. **110**, 517 (1984).

³S. M. Heald and E. A. Stern, Phys. Rev. B **16**, 5549 (1977).

⁴J. E. Fischer and T. E. Thompson, Phys. Today **31**, 36 (1980).

⁵D. Denley, P. Perfetti, R. S. Williams, D. A. Shirley, and J. Stöhr, Phys. Rev. B **21**, 2267 (1980).

⁶B. M. Kincaid, A. E. Meixner, and P. M. Platzman, Phys. Rev. Lett. **40**, 1296 (1978).

⁷E. J. Mele and J. Ritsko, Phys. Rev. Lett. **43**, 68 (1979).

⁸R. C. Tatar and S. Rabii, Phys. Rev. B **25**, 4126 (1982).

⁹R. F. Willis, B. Fitton, and G. S. Painter, Phys. Rev. B **9**, 1926 (1974).

¹⁰G. S. Painter and D. E. Ellis, Phys. Rev. B **1**, 4747 (1970).

¹¹A preliminary version of this work appeared in *EXAFS and Near Edge Structure III*, edited by K. O. Hodgson, B. Hedman, and J. E. Penner-Hahn (Springer-Verlag, Berlin, 1984), p. 70.

¹²A. Bianconi, Appl. Surf. Sci. **6**, 392 (1980).

¹³A. P. Hitchcock and C. E. Brion, J. Electron Spectrosc. Relat. Phenom. **18**, 1 (1980).

¹⁴F. R. McFeely, S. P. Kowalczyk, L. Ley, R. Cavell, R. A. Pollack, and D. A. Shirley, Phys. Rev. B **9**, 5268 (1974).

¹⁵D. Norman, J. Stöhr, R. Jaeger, P. J. Durham, and J. B. Pendry, Phys. Rev. Lett. **51**, 2052 (1983).